

Finite-temperature flexoelectricity in ferroelectric thin films from first principles

I. Ponomareva

Department of Physics, University of South Florida, Tampa, Florida 33620, USA

A. K. Tagantsev

Ceramics Laboratory, Swiss Federal Institute of Technology (EPFL), CH-1015 Lausanne, Switzerland

L. Bellaïche

Institute for Nanoscience and Engineering and Physics Department, University of Arkansas, Fayetteville, Arkansas 72701, USA

(Received 17 February 2012; published 5 March 2012)

A first-principles-based effective Hamiltonian technique is developed to study flexoelectricity in $(\text{Ba}_{0.5}\text{Sr}_{0.5})\text{TiO}_3$ thin films of different thicknesses in their paraelectric phase. The magnitude as well as sign of individual components of the flexoelectric tensor are reported, which provides answers to existing controversies. The use of this numerical tool also allows us to show that flexoelectric coefficients depend strongly on the film's thickness and temperature. Such dependence is explained using the relationship between the flexoelectric coefficients and the dielectric susceptibility.

DOI: [10.1103/PhysRevB.85.104101](https://doi.org/10.1103/PhysRevB.85.104101)

PACS number(s): 77.55.fe, 77.22.Ej, 77.65.Ly, 77.84.-s

I. INTRODUCTION

The effect of strain gradient on properties of ferroelectric films is of large scientific and technological importance. Scientific interest stems from the fact that such a gradient can give rise to *flexoelectricity*, which characterizes the coupling between the polarization and strain *gradient*. In real materials, strain gradients are virtually unavoidable due to strain relaxation and are believed to contribute to deterioration of dielectric properties.¹ Despite a large number of recent works,^{1–15} some issues related to flexoelectricity are not well understood or are even controversial. For instance, one puzzling issue concerns the order of magnitude of the flexoelectric coefficients, μ_{pqrs} , which are defined as

$$P_p = \mu_{pqrs} \frac{\partial \epsilon_{qr}}{\partial s}, \quad (1)$$

where p, q, r , and s represent Cartesian axes, P_p is the p component of the polarization, and $\partial \epsilon_{qr} / \partial s$ represents the strain gradient. It has been proposed¹⁶ that, in “normal” dielectrics, the μ_{pqrs} parameters are proportional to e/a , where e is the electronic charge and a is the lattice parameter, which provides an estimate of the order of 10^{-10} C/m. It was then suggested that, in materials with high values for the dielectric constant (such as ferroelectrics), the μ_{pqrs} parameters are also proportional to the dielectric permittivity.^{2,16,17} Such a suggestion implies that flexoelectric coefficients can be larger by 2, 3, or even 4 orders of magnitude with respect to the previous estimation of 10^{-10} C/m, which promoted much research on materials with high permittivity. Intriguingly, the pioneering series of works by Ma and Cross^{3–6,8} reported remarkably large values for the flexoelectric coefficients, namely, up to 100 $\mu\text{C}/\text{m}$ (which is 6 orders of magnitude larger than the aforementioned previous first estimate) in ferroelectric and relaxor ceramics. However, recent experiments on high-quality single-crystal SrTiO_3 ¹⁰ yielded only moderate coefficients of up to 9 nC/m. One has also to realize that, experimentally, only the so-called *effective* flexoelectric coefficients are available and that the individual components of the flexoelectric tensor

can be deduced only within an order of magnitude. In fact, even the sign of μ_{pqrs} is challenging to measure.¹⁰ Another open question is to know if the μ_{pqrs} parameters are dependent on the film's thickness. Accurate simulations are thus needed to better understand flexoelectricity. Moreover, being able to investigate flexoelectricity at *finite temperature* is highly desirable since such an effect is most useful above the Curie point (as a matter of fact and unlike piezoelectricity and pyroelectricity, flexoelectricity can induce a polarization in the nominal paraelectric phase, with no resulting hysteresis and with no need to pole the system). In other words, a numerical tool offering the accuracy and deep insight of first principles while overcoming its shortcomings (namely, the possibility of treating finite temperature and large supercells) may lead to a deeper knowledge of flexoelectricity. We are not aware that such a numerical tool currently exists.

In this paper we develop a first-principles-based approach that allows the study of flexoelectricity in ferroelectric thin films at finite temperature and for different films' thicknesses. Such a scheme yields a positive sign for all investigated flexoelectric coefficients in the nominal paraelectric phase, thus providing a definite answer to a previously opened question. It also predicts values of the order of 2–20 nC/m for these coefficients, therefore giving an answer to another controversial issue. Finally, this newly developed numerical tool reveals a strong dependency of flexoelectric coefficients on films' thickness (as well as on temperature). Such dependency can be understood from the relationship between the flexoelectric coefficients and the dielectric susceptibility of the film.¹⁷

This paper is organized as follows. Section II describes the presently developed scheme to compute finite-temperature flexoelectricity. In Sec. III, we present and analyze the results of the simulations. Finally, Sec. IV provides a summary and conclusion of this study.

II. METHODS

Here we simulate thin films made of disordered $(\text{Ba}_{0.5}\text{Sr}_{0.5})\text{TiO}_3$ (BST) solid solutions, mostly because

experimental data for the effect of strain gradients on properties of $(\text{Ba}_{1-x}\text{Sr}_x)\text{TiO}_3$ systems are already available.^{1,6,10,18} The studied films are mimicked to be grown along the [001] pseudocubic direction and to have AO-terminated surfaces (where A atoms are either Ba or Sr). The z axis is chosen to be along the growth direction while the x and y axes lie along the pseudocubic [100] and [010] directions, respectively. We concentrate on two different films' thickness: 6.6 nm (which is representative of ultrathin films) and 12 nm (which corresponds to thicker films). These two films are modeled by a $12 \times 12 \times m$ supercell, with $m = 17$ and 31, respectively, and for which periodic boundary conditions are applied along the in-plane directions for the long-range dipole-dipole interactions while no such periodic boundary condition exists for the growth direction.¹⁹ These films are subject to a gradient *along the growth direction* of either the ϵ_{zz} out-of-plane strain component or the ϵ_{xx} in-plane strain component. These two kinds of strain gradients, denoted as $\partial\epsilon_{zz}/\partial z$ and $\partial\epsilon_{xx}/\partial z$, respectively, are often found in real films¹ due to strain relaxation and/or have been experimentally realized.⁹ We typically apply strain gradients with a magnitude ranging from 0.2 to 1.7 μm^{-1} , which is comparable to the strain gradients occurring near dislocations.²⁰ In our setup for $\partial\epsilon_{zz}/\partial z$, (1) the bottom (001) TiO_2 layer of the film possesses a *negative* strain ϵ_{zz} equal to $-\frac{(m-1)a_{\text{lat}}}{2}\partial\epsilon_{zz}/\partial z$, where a_{lat} is around 4 Å; (2) the top (001) TiO_2 layer of the film has a *positive* strain $\epsilon_{zz} = +\frac{(m-1)a_{\text{lat}}}{2}\partial\epsilon_{zz}/\partial z$; and (3) the ϵ_{zz} strain *linearly* varies from the bottom to the top layer, implying that the central layer is under a zero ϵ_{zz} strain. (Note that items 1–3 also apply for ϵ_{xx} with respect to $\partial\epsilon_{xx}/\partial z$ when we mimic a strain gradient of ϵ_{xx} along the growth direction.) Such setup has several advantages: It likely reproduces the experimental strain profile, in the sense that the bending of the sample is believed to yield a compressive strain at the bottom surface while generating a tensile strain at the top surface,⁹ and it provides a zero average $\langle\epsilon_{zz}\rangle$ (or $\langle\epsilon_{xx}\rangle$) strain in the system, – therefore minimizing piezoelectric contribution.

We develop an effective Hamiltonian for such films with a total energy density being given by

$$\begin{aligned} \mathcal{E}_{\text{tot}}(\{\mathbf{u}(i)\}, \eta_H, \{\epsilon(i)\}, \{\sigma(j)\}) \\ = \mathcal{E}_{\text{Heff}}(\{\mathbf{u}(i)\}, \eta_H, \{\epsilon(i)\}, \{\sigma(j)\}) + \frac{\beta}{2} \sum_i \langle \mathbf{E}_{\text{dep}} \rangle \cdot \mathbf{Z}^* \mathbf{u}(i) \\ - \frac{1}{2} \sum_i f_{pqrs} \mathbf{Z}^* u_p(i) \frac{\partial \epsilon_{qr}}{\partial s}(i), \end{aligned} \quad (2)$$

where p, q, r , and s represent Cartesian axes; \mathbf{u}_i is the so-called local mode and is centered at the Ti site i . Its product with the effective charge \mathbf{Z}^* provides the local dipole moment of the unit cell i . Here η_H is the homogeneous strain tensor,²¹ while $\{\sigma(j)\}$ represents the atomic configuration of the solid solution,²² and $\epsilon(i)$ characterizes the inhomogeneous strain tensor and is centered on Ti sites i . The zero value of both η_H and $\epsilon(i)$ corresponds to the 0 K cubic lattice constant of BST (with 50% of Ba and Sr concentrations) bulk.²² Here $\epsilon(i)$ is frozen during the simulations in order to create the strain gradients aforementioned. On the other hand, the local modes and homogeneous strain tensor are allowed to relax during the computations. The expression and first-principles-

derived parameters of $\mathcal{E}_{\text{Heff}}$ are those given in Ref. 22 for BST *bulk*, except that the dipole-dipole interactions we use here are those of Ref. 19 for thin films. This effective Hamiltonian has been shown to correctly reproduce or predict various static and dynamical properties of BST alloys.^{22–25} The second term of Eq. (2) mimics the screening of the maximum depolarizing field, $\langle \mathbf{E}_{\text{dep}} \rangle$, with the magnitude of this screening being controlled by the β coefficient. More precisely, $\beta = 1$ and 0 correspond to ideal short circuit (full screening of $\langle \mathbf{E}_{\text{dep}} \rangle$) and open circuit (no screening of $\langle \mathbf{E}_{\text{dep}} \rangle$) electrical boundary conditions, respectively. A value of β in between describes a situation for which a residual depolarizing field exists. We use here $\beta = 0.98$ since it provides good agreement with experimental data in nanostructures.²⁶ Technically $\langle \mathbf{E}_{\text{dep}} \rangle$ is calculated at an atomistic level.¹⁹ The last term of Eq. (2) is used here for the first time in an effective Hamiltonian scheme, while it is analogous to an expression that has been previously introduced¹⁶ for phenomenological modeling of flexoelectricity. The f_{pqrs} parameters appearing in that term are the so-called flexocoupling coefficients.²⁷ They are computed in a series of *ab initio* calculations that utilize the density functional theory with the local density approximation,^{28,29} as well as the Vanderbilt ultrasoft pseudopotentials with a 25 Ry cutoff³⁰ and the virtual crystal approximation³¹ to model a BST bulk having Ba and Sr concentrations of 50% each. In these calculations the atoms are displaced from their ideal cubic positions by a vector that corresponds to the sum of the displacements originating from the strain gradients $\frac{\partial \epsilon_{qr}}{\partial s}(i)$ and of the displacements associated with the local mode vectors $\mathbf{u}(i)$. Typically, we used 10- and 20-atom supercells that are periodic in all three directions, with both the local modes and strain gradients changing their signs within these supercells [in order to provide a nonzero contribution to the last term of Eq. (2) while still maintaining the three-dimensional periodicity of the whole supercells]. An example of our setup to calculate f_{zxzx} is given in Fig. 1. The forces on the atoms obtained from these calculations are then used to compute

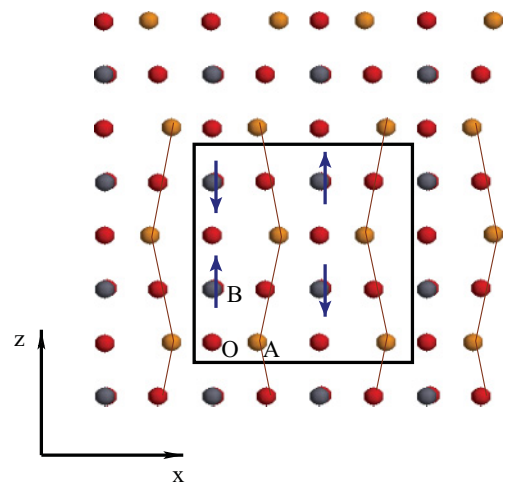


FIG. 1. (Color online) Example of atomic arrangement used in first-principles computations to extract the f_{zxzx} parameter of Eq. (1). The thick solid line shows the supercell. The arrow schematically represents the direction of the local mode u_z . The thin solid line indicates the strain gradient.

the force acting on a local mode centered on a particular Ti site, which allows the determination of the f_{pqrs} coefficients from first principles. As a result of the cubic symmetry of the reference state for the effective Hamiltonian technique, there are only three independent f_{pqrs} components: f_{zzzz} , f_{zxzx} , and f_{xxzx} . Their extracted values are $f_{zzzz} = 5.12$ V and $f_{zxzx} = 3.32$ V, while f_{xxzx} is estimated to be around 0.045 ± 0.015 V (f_{xxzx} is thus much smaller than the other two coefficients, which explains why we neglect it in the following). Note that the f_{pqrs} parameters are ground-state quantities of *bulk* systems since we used supercells that are periodic along any of the three directions to determine them at $T = 0$ K. Note also that we model flexoelectricity through the coupling between strain gradient and local dipole inside *one* unit cell (that is, it does not involve any explicit collaboration between different unit cells). Such an assumption may result in some inaccuracy for the reported f_{pqrs} flexocoupling coefficients. The total energy provided by Eq. (2) is then used in Monte Carlo simulations based on the Metropolis algorithm, in order to obtain properties of thin films subject to a strain gradient.

III. RESULTS OF THE SIMULATIONS

Let us now turn to the effective Hamiltonian simulations to determine the μ_{pqrs} coefficients of the flexoelectric tensor [see Eq.(1)], which is of rank four, in the two chosen BST films in their nominal paraelectric phase (i.e., in the phase that does not exhibit any polarization when no strain gradient is applied).³² We investigate μ_{zzzz} and μ_{zxzx} in both the studied thin and thick films, for different temperatures above the critical temperatures. Note that the Curie temperature T_C of the 6.6 nm- and 12 nm-thick film is numerically found to be equal to 300 and 235 K, respectively. The enhancement of T_C occurring when the film's thickness decreases arises from a surface effect associated with the chosen electrical boundary conditions within the present effective Hamiltonian scheme.³³ To practically compute the μ_{pqrs} flexoelectric coefficients, different magnitudes of the relevant strain gradient are applied, and the relevant component of the polarization is plotted as a function of such magnitude, as done in Fig. 2 for different temperatures in the thicker film under $\partial\epsilon_{xx}/\partial z$. The slope of this function provides the desired coefficient.

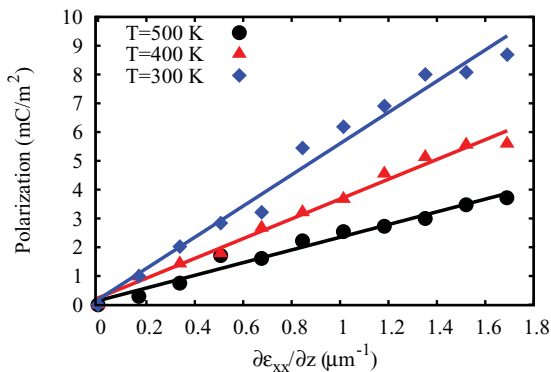


FIG. 2. (Color online) Dependence of the out-of-plane polarization component of the thicker investigated film on the strain gradient $\partial\epsilon_{xx}/\partial z$ at three temperatures. The error bar for the polarization values is smaller than the symbol size.

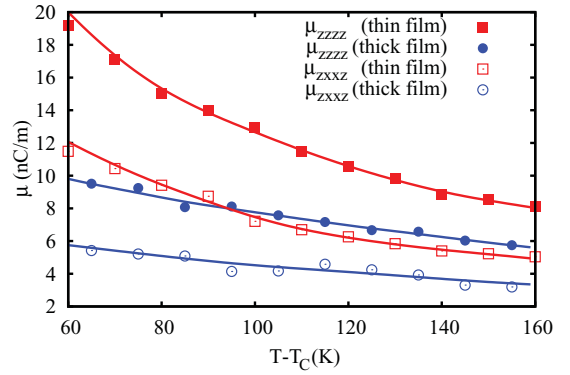


FIG. 3. (Color online) Temperature dependency of the flexoelectric coefficients in the nominal paraelectric phase of the thin and thick films. T is the temperature; T_C is the Curie temperature of the films under no strain gradient.

Figure 3 shows the dependence of the flexoelectric coefficients versus $T - T_C$ for both the thick and thin films, where T is the temperature and T_C is the Curie temperature for the films under no strain gradient. These coefficients are temperature dependent in both films and increase when getting closer to T_C as consistent with measurements.^{3-6,8,10} Figure 3 also shows that, in both films, μ_{zzzz} and μ_{zxzx} coefficients are both positive above the Curie point, which confirms the results of some works^{3-6,8,10} while contradicting other data.^{10,13} It further reports that the predicted flexoelectric coefficients typically range between a few nC/m and up to 20 nC/m, which agree rather well with the ones reported for single crystals of SrTiO₃ (1–10 nC/m) at room temperature¹⁰ while being orders of magnitude smaller than the values reported for BST ceramics.^{6,18} Such a large difference in flexoelectric coefficients between single crystals and ceramics points toward the enhanced role of surface and/or size effects on flexoelectricity (as also argued in Ref. 10). Figure 3 also reveals that the thinner film is predicted to have twice as larger flexoelectric coefficients than the thicker film. However, these latter results showing a strong thickness dependency of the flexoelectric coefficients seem at odds with the fact that the “only” flexoelectric interactions included in Eq. (2) are *bulk-like*, since the f_{pqrs} parameters were determined by first-principles calculations performed on structures that are periodic in all three Cartesian directions. As we will see below, such a seemingly contradictory fact can be easily resolved and understood. For that, let us rewrite Eq. (1) as¹⁷

$$P_p = \frac{1}{2} \chi_{tp} \epsilon_0 h_{tqrs} \frac{\partial \epsilon_{qr}}{\partial s}, \quad (3)$$

where p , t , q , r , and s represent Cartesian axes, χ_{tp} is a component of the dielectric susceptibility, and ϵ_0 is the dielectric permittivity of free space. (Note that the factor $\frac{1}{2}$ appearing in Eq. (3) originates from the factor $\frac{1}{2}$ occurring in front of the last energetic term of Eq. (2).) In Eq. (3) h_{tqrs} is defined as being equal to the ratio $2\mu_{pqrs}/\chi_{tp}\epsilon_0$. Interestingly we numerically found that h_{zzzz} and h_{zxzx} are nearly independent of not only the temperature but also of the film's thickness. For instance, we numerically obtain a value of 2.8 and 3.0 V for the h_{zxzx} coefficient of the thin and thick film, respectively, for any temperature above T_C . This

reveals that (1) thickness and temperature effects constitute a rather negligible effect when focusing on h_{zxxz} rather than on μ_{zxxz} ; (2) the large difference shown in Fig. 3 between the μ_{zxxz} coefficients of the thick and thin films mostly comes from their large difference in dielectric susceptibility; and (3) the temperature dependency of μ_{zxxz} fully originates from the (“usual”) temperature dependence of the χ_{33} dielectric susceptibility. Similar conclusions are also reached for the μ_{zzzz} coefficients since h_{zzzz} is numerically found to be 5.0 and 5.2 V for the thin and thick film, respectively, for any investigated temperature. Moreover, the aforementioned values of h_{zxxz} and h_{zzzz} are very close to the values of the bulk flexocoupling coefficients f_{zxxz} (equal to 3.32 V) and f_{zzzz} (equal to 5.12 V), respectively, that were extracted from first principles and used in the third term of Eq. (1). In other words, our present calculations and analysis reveal that the μ_{pqrs} flexoelectric coefficients of any thin film and at any temperature can be better understood and well approximated by using the relation $\mu_{pqrs} = \frac{1}{2} f_{pqrs} \chi_{tp} \epsilon_0$, with f_{pqrs} being the so-called flexocoupling coefficient (which is independent of both temperature and thickness, as a result of being a ground-state bulk property) while the temperature dependency and thickness dependency of the μ_{pqrs} coefficients mostly originate from the dielectric susceptibility.

IV. CONCLUSIONS

In summary, we developed a first-principles-based approach to simulate flexoelectricity in ferroelectric thin films. Specific advantages of such approach are (1) the possibility to independently calculate the *magnitude but also sign of different* components of the flexoelectric coefficients tensor; (2) that no empirical input is required; (3) the possibility to study the dependency of flexoelectric coefficients on several important parameters, such as *temperature* and *film’s thickness*;

(4) the determination of the “pure” flexoelectric effect, that is, without the contribution from ferroelastic domains that are usually present in any grown sample; and (5) a deep insight provided by such method and the analysis of its results. Our simulations provide values ranging between a few nC/m and up to 20 nC/m, and positive sign of the flexoelectric coefficients. They also reveal and explain their strong dependency on the film’s thickness and temperature, because of the indirect effect involving the dielectric susceptibility. (Note that investigating the role of surface effects other than those included here (such as surface-induced change of hybridization or surface relaxation) on flexoelectricity can be, in principle, incorporated by our scheme via the addition of novel energetic terms in Eq. (2). This incorporation is beyond the scope of the present work but may constitute the basis of a future study.)

ACKNOWLEDGMENTS

We thank Raffaele Resta for insightful comments on the manuscript. I.P. acknowledges the US Department of Energy, Office of Basic Energy Sciences, under Award DE-SC0005245 (for computational studies) and USF under Grant No. R070699 (for some theoretical developments). L.B. thanks support from by NSF grants DMR-1066158 and DMR-0701558. L.B. also thanks ARO Grant W911NF-12-1-0085, ONR Grants N00014-11-1-0384, N00014-08-1-0915, and N00014-07-1-0825 (DURIP), and the Department of Energy, Office of Basic Energy Sciences, under contract ER-46612 for discussions with scientists sponsored by these grants. A.K.T. thanks financial support from Swiss National Science Foundation. The use of services provided by Research Computing, USF, are greatly acknowledged. Some computations were also made possible due to the MRI Grant 0722625 from NSF.

¹G. Catalan, B. Noheda, J. McAneney, L. J. Sinnamon, and J. M. Gregg, *Phys. Rev. B* **72**, 020102 (2005).

²A. K. Tagantsev, *Phys. Rev. B* **34**, 5883 (1986).

³W. Ma and L. Cross, *Appl. Phys. Lett.* **78**, 2920 (2001).

⁴W. Ma and L. Cross, *Appl. Phys. Lett.* **79**, 4420 (2001).

⁵W. Ma and L. Cross, *Appl. Phys. Lett.* **82**, 3293 (2003).

⁶W. Ma and L. Cross, *Appl. Phys. Lett.* **81**, 3440 (2002).

⁷G. Catalan, L. Sinnamon, and J. Gregg, *J. Phys. Condens. Matter* **16**, 2253 (2004).

⁸W. Ma and L. Cross, *Appl. Phys. Lett.* **88**, 232902 (2006).

⁹L. Cross, *J. Mater. Sci.* **41**, 53 (2006).

¹⁰P. Zubko, G. Catalan, P. R. L. Welche, A. Buckley, and J. F. Scott, *Phys. Rev. Lett.* **99**, 167601 (2007).

¹¹M. Majdoub, P. Sharma, and T. Cagin, *Phys. Rev. B* **77**, 125424 (2008).

¹²E. A. Eliseev, A. N. Morozovska, M. D. Glinchuk, and R. Blinc, *Phys. Rev. B* **79**, 165433 (2009).

¹³R. Maranganti and P. Sharma, *Phys. Rev. B* **80**, 054109 (2009).

¹⁴R. Resta, *Phys. Rev. Lett.* **105**, 127601 (2010).

¹⁵J. Hong, G. Catalan, J. F. Scott, and E. Artacho, *J. Phys. Condens. Matter* **22**, 112201 (2010).

¹⁶S. M. Kogan, *Sov. Phys. Solid State* **5**, 2069 (1964).

¹⁷A. K. Tagantsev, *Phase Transit.* **35**, 119 (1991).

¹⁸J. Y. Fu, W. Zhu, N. Li, and L. E. Cross, *J. Appl. Phys.* **100**, 024112 (2006).

¹⁹I. Ponomareva, I. I. Naumov, I. Kornev, H. Fu, and L. Bellaiche, *Phys. Rev. B* **72**, 140102 (2005).

²⁰M.-W. Chu, I. Szafraniak, R. Scholz, C. Harnagea, D. Hesse, M. Alexe, and U. Gsele, *Nat. Mater.* **3**, 87 (2004).

²¹W. Zhong, D. Vanderbilt, and K. M. Rabe, *Phys. Rev. B* **52**, 6301 (1995).

²²L. Walizer, S. Lisenkov, and L. Bellaiche, *Phys. Rev. B* **73**, 144105 (2006).

²³Q. Zhang and I. Ponomareva, *Phys. Rev. Lett.* **105**, 147602 (2010).

²⁴I. Ponomareva, L. Bellaiche, T. Ostapchuk, J. Hlinka, and J. Petzelt, *Phys. Rev. B* **77**, 012102 (2008).

²⁵J. Hlinka, T. Ostapchuk, D. Nuzhnyy, J. Petzelt, P. Kuzel, C. Kadlec, P. Vanek, I. Ponomareva, and L. Bellaiche, *Phys. Rev. Lett.* **101**, 167402 (2008).

- ²⁶L. Louis, P. Gemeiner, I. Ponomareva, L. Bellaiche, G. Geneste, W. Ma, N. Setter, and B. Dkhil, [Nano Lett.](#) **10**, 1177 (2010).
- ²⁷E. A. Eliseev, A. N. Morozovska, M. D. Glinchuk, and R. Blinc, [Phys. Rev. B](#) **79**, 165433 (2009).
- ²⁸P. Hohenberg and W. Kohn, [Phys. Rev.](#) **136**, B864 (1964).
- ²⁹W. Kohn and L. J. Sham, [Phys. Rev.](#) **140**, A1133 (1965).
- ³⁰D. Vanderbilt, [Phys. Rev. B](#) **41**, 7892 (1990).
- ³¹L. Bellaiche and D. Vanderbilt, [Phys. Rev. B](#) **61**, 7877 (2000).
- ³²The fact that all the components of the $\epsilon(i)$ tensors are frozen in our simulations implies that there is an “effective” clamping at the level of unit cells. This constraint can be removed by allowing some

components of $\epsilon(i)$ to relax. In this case, however, the $\partial\epsilon_{zz}/\partial z$ gradient will induce a gradient $\partial\epsilon_{xx}/\partial z$ (and vice versa), which will lead to a coupling between different flexoelectric coefficients. While such “effective” clamping is not expected to play a role in the flexoelectric polarization induced by a given strain profile, it can contribute to the overall polarization for temperatures below the paraelectric-to-ferroelectric transition because of local piezoelectric couplings. This explains why we decided to focus on flexoelectricity in the nominal paraelectric phase, since no piezoelectric coupling exists for this phase.

- ³³P. Ghosez and K. M. Rabe, [Appl. Phys. Lett.](#) **76**, 2767 (2000).